A NEW METHOD FOR AUTOMATIC SEGMENTATION OF ENDOCARDIAL BOUNDARIES IN ECHOCARDIOGRAPHIC SEQUENCES

C. Corsi, F. Veronesi, A. Sarti and C. Lamberti

DEIS, University of Bologna, Bologna, Italy

ccorsi@deis.unibo.it

Abstract: This study presents a geometric model for automatic segmentation of left ventricular (LV) boundaries throughout the cardiac cycle in echocardiographic images. The segmentation is obtained by solving a partial differential equation that describes a motion under geodesic curvature. The initial condition for the partial differential equation is computed by applying a maximum likelihood segmentation of the endocardium based on the density probability distribution of the gray levels of the image as well as smoothness constraints. To model gray level behavior of ultrasound images the classic Rayleigh probability distribution is considered. The initial condition is automatically computed for each image throughout the cardiac cycle and the dynamic segmentation of the LV boundary is automatically achieved. Preliminary experiments were conducted with satisfactory segmentation outcomes in comparison with expert manual tracing. The proposed method is fast, no operator-dependent and allows easy noninvasive serial segmentation of endocardial boundaries throughout the cardiac cycle.

Introduction

Quantification of global left ventricular (LV) function is a strong clinical need for the evaluation of cardiac diseases because it has important diagnostic and therapeutic implications. Noninvasive modalities to evaluate global LV function include echocardiography, cardiovascular magnetic resonance (CMR) and single photon emission computed tomography (SPECT). All these techniques have been shown to agree well with invasively acquired LV function assessment by angiography [1][2][3]. Compared to CMR and SPECT, echocardiography is low cost and portable and it is the most widely used imaging modality for the analysis of global LV function.

For an accurate evaluation of LV function endocardial visualization is essential. Unfortunately, in many cardiac patients, echocardiographic images show poor image quality that does not allow consistent endocardial visualization and tracking of the blood-tissue interface. Speckling effects greatly reduce the observable details within such images and boundaries between different cardiac structures are not well defined. Therefore echocardiographic images are particularly difficult to process and their quality is usually too low to reliably detect features locally.

Classical segmentation techniques usually fail when applied to echocardiographic images for LV endocardial contour detection. However, continuing efforts directed towards improving endocardial visualization made by both echocardiographic imaging equipment manufacturers and researchers have recently produced new and effective quantitative approaches for the detection of LV endocardial contours from echocardiographic images. These approaches are based on different methods: multidimensional space-frequency methods [4][5], Markov random fields [6][7], neural networks [8], fuzzy logic [9][10], active contours [11] and level set models [12][13][14]. To improve the performance of LV segmentation and to fill the lack of information due to the presence of noise on these data, the proposed methods are semi-automatic or require a prior anatomical LV shape knowledge. Semi-automatic approaches have the limitation of requiring the operator intervention which is a subjective and time-consuming procedure while the use of prior anatomical LV shape knowledge could introduce errors due to variability of anatomical shapes and particularly in patients with odd-shaped ventricles [1][15].

The aim of this study was to develop a model for automatic segmentation of echocardiographic data throughout the cardiac cycle without any assumption regarding the LV shape. Accordingly, in this study we present a novel method for automatic segmentation of endocardial boundaries in echocardiographic sequences. The proposed method is based on a mathematical model [16] described by a partial differential equation (PDE) that characterizes the motion of a curve towards the endocardial boundaries. The initial condition for the PDE is obtained applying a rough segmentation of the endocardium by considering a region-based approach and embedding in the model the knowledge of the statistical distribution of gray levels in ultrasound data [17]. This approach allows automatic segmentation of echocardiographic images for dynamic detection of LV endocardial boundaries without prior anatomical LV shape knowledge.

Preliminary experiments to evaluate the performance of the developed model were conducted on short axis two-dimensional echocardiographic images with satisfactory segmentation outcomes in comparison with manual tracing.

ISSN: 1727-1983

Materials and Methods

In problems of curve evolution, the level set method and particularly the motion by mean curvature introduced by Osher and Sethian [18] has been extensively used. Being designed to handle problems in which interfaces develop corners, cusps and changes in topology, it presents several advantages over many other techniques. In [18] Osher and Sethian represent a curve C_1 via a Lipschitz function Ψ, by $C_1=\{(x,y)|\ \Psi(x,y)=0\}$, and the evolution of the curve is given by the zero-level curve at time t of the function $\Psi(x,y,t)$.

Evolving the curve C_1 in normal direction with speed F amounts to solve the following differential equation [18]:

$$\begin{cases} \dfrac{\partial \Psi}{\partial t} = F|\nabla \Psi| \\ \Psi(x,y,0) = \Psi_0(x,y) \end{cases} \tag{1}$$

where the function $\Psi_0(x,y)$ defines the initial contour.

A particular case is the motion by geodesic curvature:

$$\begin{cases} \dfrac{\partial \Psi}{\partial t} = gK|\nabla \Psi| + \nabla g \cdot \nabla \Psi & \text{in } \Omega \times]0,\infty[\\ \Psi(x,y,t) = \min \Psi_0(x,y) & \text{in } \partial\Omega \times]0,\infty[\\ \Psi(x,y,0) = \Psi_0(x,y) & \text{in } \Omega \end{cases} \tag{2}$$

where $\Psi(x,y,t)$ represents the level set function that embeds the contour as its zero level and Ω represents the image domain. The term $gK|\nabla\Psi|$ leads the curve to move in the normal direction with a speed equal to the Euclidean curvature K weighted by the function g; $\nabla g \cdot \nabla \Psi$ is a passive motion in the direction of the velocity field $-\nabla g$. The surface evolution described with equations (2) will have a steady state solution when the two terms balance each other.

The function g is an edge indicator [19] computed on a smoothed version of the image $I:\Omega \subset \Re^2 \to \Re$, obtained applying a geodesic filter:

$$g(x,y) = \left[1 + \left(\frac{I_{smooth}}{\beta}\right)^2\right]^{-1} \tag{3}$$

The local edge indicator g(x,y) is a non-increasing function: the value of g is closer to 1 in flat areas and closer to 0 in areas with large changes in image intensity. By viewing g as a potential function, we note that its minima denote the position of edges. Also, the gradient of this potential function is a force field that always points in the local edge direction.

The initial condition Ψ_0 for the curve evolution described in (2) is computed in a previous step in which a rough endocardium contour is obtained by applying a region-based PDE [17].

In the formulation of the region-based PDE we embedded the knowledge of the statistical distribution of gray levels in ultrasound data, assumed to be uncorrelated and independently distributed and characterized by their respective probability density. A closed curve C_2 divides the image domain in an "inside" Ω_i and an "outside" Ω_e region; $P_i=\prod\Omega_i(C_2)p(I)$ is the probability of the random field inside the curve and $P_e=\prod\Omega_e(C_2)p(I)$ is the probability outside the curve. Without any a priori knowledge about the shape of the object to be detected, we look for the curve C_2 that maximizes the likelihood function given by the product of the inner and the outer probability [20]: $P[I|C_2]=P_i\,P_e$. Since the log function is strictly increasing, the maximum value of $P[I|C_2]$, if it exists, will occur at the same points as the maximum value of $l(I,C_2)=\log(P[I|C_2])$. This function is the "log-likelihood" and in many cases it is easier to work with it than with the likelihood function. To perform a maximum likelihood segmentation of the target, we need to maximize the functional l with respect to variation of the curve C_2. By considering the Rayleigh noise distribution: $p(I)_{Rayleigh}=I(x,y)/\sigma^2\exp(-I(x,y)^2/\sigma^2)$, the corresponding log-likelihood is given by [22]:

$$\begin{aligned} l(I,C) &= \log P_i + \log P_e = \\ &= \int_{\Omega_i(C)} \log p(I)dxdy + \int_{\Omega_e(C)} \log p(I)dxdy = \\ &= A_i \log\left(\frac{1}{A_i}\int_{\Omega_i(C)} I(x,y)^2 dxdy\right) + A_e \log\left(\frac{1}{A_e}\int_{\Omega_e(C)} I(x,y)^2 dxdy\right) \end{aligned} \tag{4}$$

where A_i e A_e are respectively the number of pixels in Ω_i and Ω_e and the parameters of the probability density function (pdf) have been estimated following [21].

In order to obtain a well-posed and well-conditioned problem we need to introduce a regularization in the shape of the curve. To this scope, a length term has been introduced, and finally we ask to minimize the functional:

$$\begin{aligned} F = \mu(\text{length}(C)) - A_i \log\left(\frac{1}{A_i}\int_{\Omega_i(C)} I(x,y)^2 dxdy\right) + \\ + A_e \log\left(\frac{1}{A_e}\int_{\Omega_e(C)} I(x,y)^2 dxdy\right) \end{aligned} \tag{5}$$

where $\mu \geq 0$.

The associated Euler-Lagrange equation results:

$$0 = \delta(\Psi)\left[\begin{aligned} &\mu \operatorname{div}\left(\frac{\nabla\Psi}{|\nabla\Psi|}\right) + \\ &+\log\left(\frac{1}{A_i}\int_{\Omega_i} I^2 dxdy\right) + \frac{A_i I^2 - \int_{\Omega_i} I^2 dxdy}{\int_{\Omega_i} I^2 dxdy} - \\ &-\log\left(\frac{1}{A_e}\int_{\Omega_e} I^2 dxdy\right) - \frac{A_e I^2 - \int_{\Omega_e} I^2 dxdy}{\int_{\Omega_e} I^2 dxdy} \end{aligned}\right] \tag{6}$$

ISSN: 1727-1983

In level set methods, the Euler-Lagrange equation for Ψ acts only locally, on a few level curves around Ψ=0. To extend the evolution to all level sets of Ψ we replace $\delta(\Psi)$ with $|\nabla\Psi|$. Thus equation (6) will act on all the level curves, of course stronger on the zero level curve.

From (6), we simply get the associated flow described by the following equations:

$$\partial_t \Psi = |\nabla\Psi| \left[\begin{array}{l} \mu \mathrm{div}\left(\frac{\nabla\Psi}{|\nabla\Psi|}\right) + \\ + \log\left(\frac{1}{A_i}\int_{\Omega_i} I^2 dxdy\right) + \frac{A_i I^2 - \int_{\Omega_i} I^2 dxdy}{\int_{\Omega_i} I^2 dxdy} - \\ - \log\left(\frac{1}{A_e}\int_{\Omega_e} I^2 dxdy\right) - \frac{A_e I^2 - \int_{\Omega_e} I^2 dxdy}{\int_{\Omega_e} I^2 dxdy} \end{array} \right]$$

$$\Psi(x,y,0) = \Psi_{00}(x,y)$$

$$\frac{\delta(\Psi)\partial\Psi}{|\nabla\Psi|\partial n} = 0 \qquad (7)$$

where $\Psi(x,y,0)$ is an initial function with the property that its zero level set corresponds to the position of the initial front and the third equation represents the boundary conditions. The evolution process will stop when the region probability terms of the inside regions do equal the terms of outside regions, up to regularization of the boundaries.

To perform the endocardium segmentation, the operator selects one point inside the endocardium in one image. Automatically a surface whose zero level is a circle having as center the selected point is built and it is used as Ψ_{00}, the initial condition for equations (7). When the evolution process stops the undesired detected areas outside and inside the LV chamber are automatically removed from the resulted zero level set function. This deletion does not require any manual intervention and it is fully automated since the coordinates of the initial selected point are known. The resulting curve is the initial condition for the motion under geodesic curvature, Ψ_0, described by equations in (2). The final result of this evolution represents the endocardial boundary for that image.

The same procedure is automatically applied to each consecutive image throughout the cardiac cycle, by considering the same initial point, resulting in automatic segmentation of endocardial boundaries in the echocardiographic sequence.

This method was tested on nine short axis transthoracic two-dimensional echocardiographic sequences acquired with a SONOS 7500 system (Philips) equipped with a 2D probe.

To evaluate the reliability of the automated detected contours, they were reviewed by an experienced echocardiographer for a qualitative evaluation. In addition the expert manually traced the endocardial contours on the same images. The areas inside the manually and automatically detected contours were compared by linear regression and Bland-Atman analysis.

The reproducibility of the automated detection was tested in two subjects by repeating the analysis throughout the cardiac cycle twice: the area-time curve was extracted and the variability of the frame-by-frame derived measurements was calculated as the absolute difference between the repeated measurements in percent of their mean. Paired t-test was used to test the significance of the differences between the repeated measurements.

Results

The simulation were performed in Matlab 6.1. The operator selects one point in the image and the time required to analyze a single image is less than 30 seconds. Analysis of the entire cardiac cycle adds additional 30 seconds for every subsequent frame.

In Figure 1 we show three steps required for the endocardium segmentation.

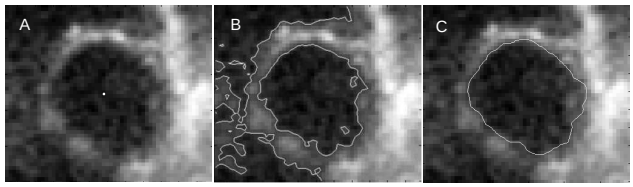

Figure 1: (A) Initial point selection; (B) Result of the maximum likelihood segmentation; (C) Final detected endocardial contour.

Examples of extracted contours throughout the cardiac cycle are shown in Figure 2 and in Figure 3.

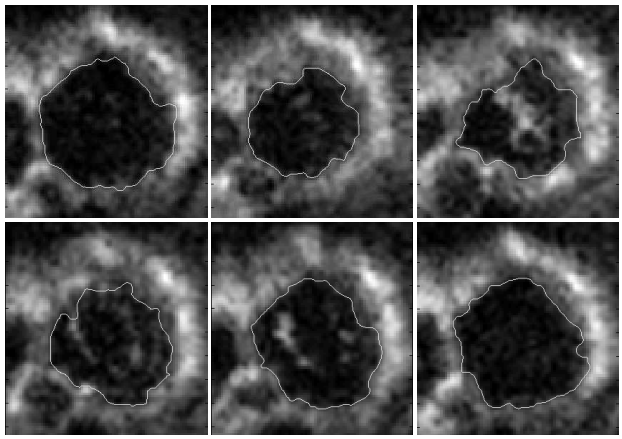

Figure 2: Examples of the detected endocardial contours in one plane throughout the cardiac cycle.

ISSN: 1727-1983

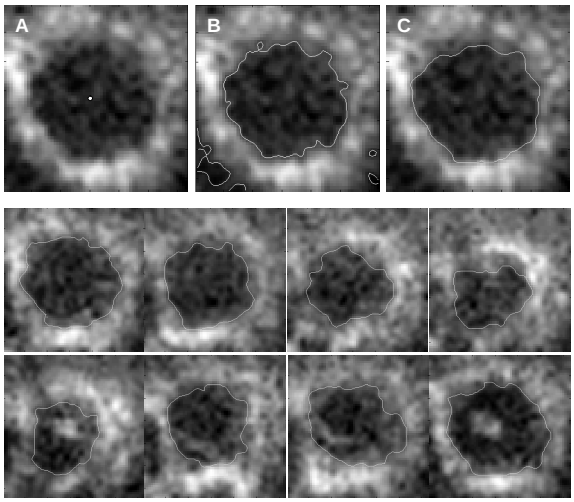

Figure 3: Examples of the detected endocardial contours throughout the cardiac cycle. Top panels: (A) initial point selection in one frame; (B) result of the maximum likelihood segmentation; (C) final detected endocardial contour. Bottom panels: automated detected endocardial contours throughout the cardiac cycle.

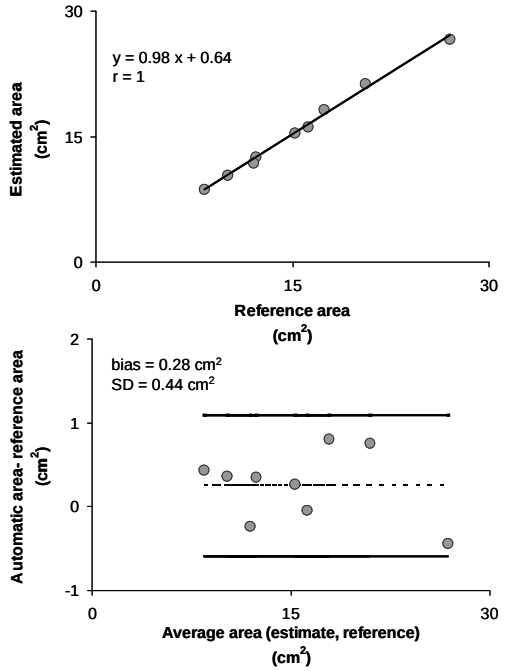

Figure 4: Linear regression and Bland-Altman analyses between the automated detected area compared to the reference area.

The outcomes of the segmentation satisfied the experienced echocardiographer. Linear regression analysis (Figure 4, top panel) between the automated detected area and the reference area resulted in excellent correlation coefficients (r=1) and regression slope (y=0.98x+0.64). Bland-Altman analysis (Figure 4, bottom panel) showed no significant bias (bias=0.28 cm^2) between the automated area measurements and the reference values reflecting a systematic error of 1.61%

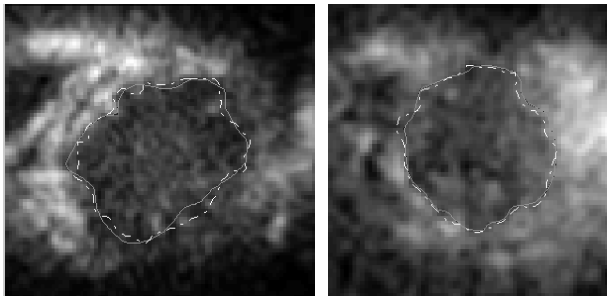

Figure 5: Examples of the detected contours obtained by the automated technique (dashed line) compared to the manually traced (solid line).

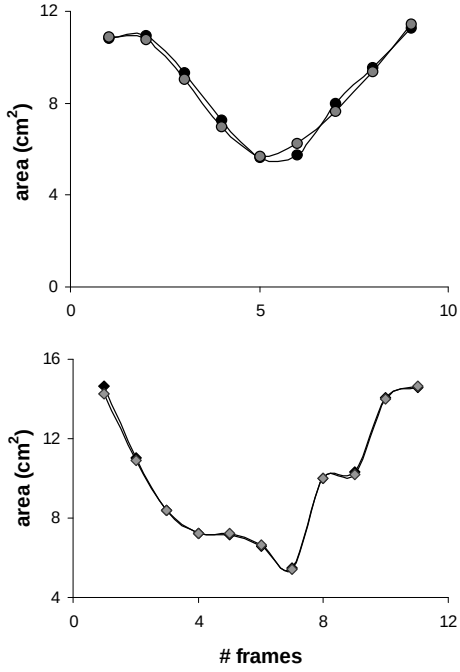

Figure 6: Area-time curves obtained in two planes throughout the cardiac cycle by repeating twice the analysis.

of the corresponding mean values and narrow 95% limit of agreement (2SD=0.88cm^2). Two examples of the good correspondence between the manually traced and automated detected contours are shown in Figure 5.

The computed inter-measurements variability resulted in 1.7%. Two examples of the area-time curves automatically extracted twice for a mid LV acquisition (top panel) and a basal LV acquisition (bottom panel) throughout the cardiac cycle, are shown in Figure 6.

Discussion

Currently two-dimensional echocardiography is the most commonly used imaging technique to estimate LV function, which is usually performed in a subjective [22] and experience-dependent [23] manner.

Quantitative methods previously applied to two-dimensional echocardiographic images were also limited because the measurements were based on manual tracing and geometric assumptions, which

ISSN: 1727-1983

introduce errors, particularly in patients with regional wall-motion abnormalities, asymmetrically shaped ventricle, or both. In addition, these methods are time-consuming and their application is limited to end-diastolic and end-systolic frames.

Our method represents an improvement with respect to the ones used in clinical practice for different reasons. First, the method we propose automatically detects endocardial boundaries throughout the cardiac cycle and the user intervention consists in the selection of only one point inside the LV chamber. These two advantages would lead to the analysis of the LV function in the cardiac cycle and limit the subjectivity of the current analysis.

The results we obtained were positively reviewed by an expert reading and validated against manual tracing, showing excellent correspondence between the manually traced and automated detected contours.

Even if in this study we did not evaluate the reproducibility of our method, the results we obtained by simply repeating twice the analysis throughout the cardiac cycle in two planes showed very good results. These initial test also represents a first step to demonstrate the independence of our method from the initial manually selected point.

We are aware that for an exhaustive and complete evaluation of the performance of our technique, the analysis of the shape of the extracted contours in comparison to the manually traced ones, for example by the computation of the Hausdorff distance [24][25], would be necessary.

Importantly, due to the level set formulation, its implementation in the three-dimensional domain is very easy and the extraction of volume would be a natural improvement of this algorithm. The three-dimensional version of our method promises even better results since a major information would be available for the surface evolution. This improvement would be possible because nowadays, real-time 3D echocardiographic equipments that capture all heart's volume data points within a cardiac beat, are available and widely used in clinical practice.

Conclusions

In summary, we developed a novel, fast, accurate and automatic technique for segmentation and analysis of echocardiographic images throughout the cardiac cycle without any assumption regarding the LV shape. We strongly believe that automatic segmentation in its 3D implementation, together with real-time three-dimensional technology for echocardiographic acquisition will definitely represent the near future for this imaging acquisition modality.

References

[1] FOLLAND E.D., PARISI A.F., MOYNIHAN P.F., JONES D.R., FELDMAN C.L., and TOW D.E. (1979): 'Assessment of left ventricular ejection fraction and volumes by real-time, two-dimensional echocardiography: a comparison of cineangiographic and radionuclide techniques', *Circulation*, **69(4)**, pp. 760–766

[2] ICHIKAWA Y., SAKUMA H., KITAGAWA K., ISHIDA N., TAKEDA K., and UEMURA S. (2003): 'Evaluation of left ventricular volumes and ejection fraction using fast steady-state cine MR imaging: comparison with left ventricular angiography', *J Cardiovasc Magn Reson*, **5(2)**, pp. 333–342

[3] ISKANDRIAN A.E., GERMANO G., VANDECKER W., OGILBY J.D., WOLF N. and MINTZ R. (1998): 'Validation of left ventricular volume measurements by gated SPECT 99mTc-labeled sestamibi imaging', *J Nucl Cardiol*, **5(6)**, pp. 574–578

[4] MULET-PARADA M., and NOBLE J.A. (2000): '2D+T acoustic boundary detection in echocardiography', *Med. Image Analysis*, **4**, pp. 21-30

[5] ANGELINI E.D., LAINE A. F., TAKUMA S., HOLMES J.W., and HOMMA S. (2001): 'LV volume quantification via spatiotemporal analysis of real-time 3-D echocardiography', *IEEE Trans. Med. Imag.*, **6**, pp. 457–469

[6] PAPADEMETRIS X., SINUSAS A.J., DIONE D.P., and DUNCAN J.S. (2001): 'Estimation of 3D left ventricular deformation from echocardiography', *Med. Image Analysis*, **5**, pp. 17–28

[7] BOUKERROUI D., BASKURT A., NOBLE J.A., and BASSET O. (2003): 'Segmentation of ultrasound images-multiresolution 2D and 3D algorithm based on global and local statistics', *Pattern Recognition Lett.*, **24**, pp. 779–790

[8] COPPINI G., POLI R., and VALLI R. (1995): 'Recovery of 3-D shape of the left ventricle from echocardiographic images', *IEEE Trans. Med. Imag*., **14**, pp. 301–317

[9] SATAREHDAN S.K., and SORAGHAN J.J. (1999): 'Automatic cardiac LV boundary detection and tracking using hybrid fuzzy temporal and fuzzy multiscale edge detection', *IEEE Trans. Biomed. Eng.*, **46**, pp. 1364–1378

[10] SANCHEZ-ORTIZ G.I., WRIGHT G.J.T., CLARKE N., J. DECLERCK, BANNING A., and NOBLE J.A. (2002): 'Automated 3D echocardiography analysis compared with manual delineation and MUGA' *IEEE Trans. Med. Imag.*, **21(9)**, pp. 1069–1076

[11] KASS M., WITKIN A., and TERZOPOULOS D. (1988): 'Snakes: Active contour models', *Int. J. Comput. Vision*, **1**, pp. 321–331

[12] SARTI A., and MALLADI R., (1999): 'A Geometric Level Set Model for Ultrasound Image Analysis'*in Computing Sciences Directorate*, Mathematics Department, University of California, Berkeley

[13] LIN N., YU W., and DUNCAN J.S. (2003): 'Combinative multi-scale level set framework for echocardiographic image segmentation', *Med. Image Analysis*, **7(4)**, pp. 529–537

ISSN: 1727-1983

[14] PARAGIOS N., (2003): 'A level set for shape-driven segmentation and tracking of the left ventricle', *IEEE Trans. Med. Imag.*, **22(6)**, pp. 773–776

[15] WYATT H.L., MEERBAUM S., HENG M.K., GUERET P., and CORDAY E. (1980): 'Cross-sectional echocardiography. III. Analysis of mathematic models for quantifying volume of symmetric and asymmetric left ventricles', *Am Heart J.*, **100(6 Pt 1)**, pp. 821-828

[16] CHENG L., BURCHARD P., MERRIMAN B., and OSHER S. (2002): 'Motion of curves constrained on surfaces using a level-set approach', *J Comp Phys*, **175(2)**, pp. 604-644

[17] SARTI A., CORSI C., MAZZINI E., and LAMBERTI C. (2005): 'Maximum Likelihood Segmentation of Ultrasound Images with Rayleigh Distribution', *IEEE Transactions on Ultrasonics Ferroelectrics and Frequency Control*, **52(6**), pp. 947-960

[18] OSHER S., and SETHIAN J.A. (1988): "Fronts propagating with curvature-dependent speed: Algorithms based on Hamilton–Jacobi Formulation", *J. Comput. Phys.*, **79**, pp. 12–49

[19] PERONA P, and MALIK J. (1990): "Scale-space and edge detection using anisotropic diffusion", *IEEE Trans. Pattern Analysis and Machine Intelligence*, **12(7)**, pp.:629 - 639

[20] AZZALINI A. (1996): 'Statistical Inference-Based on the Likelihood', Chapman and Hall, New York.

[21] CHESNAUD C., REFREGIER P., and BOULET V. (1999): "Statistical Region Snake-Based Segmentation Adapted to Different Physical Noise Models", *IEEE Trans PAMI*, **21(11)**, pp. 1145-1157

[22] POPP R., AGATSTON A., ARMSTRONG W., NANDA N., PEARLMAN A., RAKOWSKI H., SEWARD J., SILVERMAN N., SMITH M., STEWART W., TAYLOR R., THYS D., and DAVIS C. (1998): "Recommendations for training in performance and interpretation of stress echocardiography", Committee on Physician Training and Education of the American Society of Echocardiography, *.J Am Soc Echocardiography*, **11(1)**, pp. 95-96.

[23] PICANO E., LATTANZI F., ORLANDINI A., MARINI C., and L'ABBATE A. (1991): "Stress echocardiography and the human factor: the importance of being expert", *J Am Coll Cardiol*., **17(3)**, pp. 666-669.

[24] HUTTENLOCHER D.P., KLANDERMAN G.A., and RUCKLIDGE W.J. (1993): "Comparing images using the Hausdorff distance", *IEEE Trans PAMI*, **15(9)**, pp. 850-863

[25] BELOGAY E., CABRELLI C., MOLTER U., and SHONKWILER R. (1997): "Calculating the Hausdorff distance between curves", *Information Processing Letters*, **64**, pp. 17-22

ISSN: 1727-1983